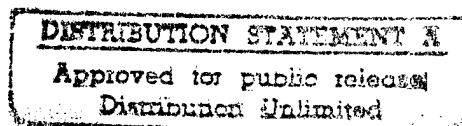


Second Annual Report on ONR Grant N-00014-93-0080

**A STUDY OF SOLID PROPELLANTS USING A MICROPROBE  
MASS SPECTROMETER SYSTEM**

Thomas A. Litzinger  
Penn State University  
210D Mechanical Engineering Bldg.  
University Park, PA 16802



19951026 079



OFFICE OF THE UNDER SECRETARY OF DEFENSE (ACQUISITION)  
DEFENSE TECHNICAL INFORMATION CENTER  
CAMERON STATION  
ALEXANDRIA, VIRGINIA 22304-6145

IN REPLY  
REFER TO

DTIC-OCC

SUBJECT: Distribution Statements on Technical Documents

TO: OFFICE OF NAVAL RESEARCH  
CORPORATE PROGRAMS DIVISION  
ONR 333  
800 NORTH QUINCY STREET  
ARLINGTON, VA 22217-5660

- 1995 1026 079
1. Reference: DoD Directive 5230.24, Distribution Statements on Technical Documents, 18 Mar 87.
  2. The Defense Technical Information Center received the enclosed report (referenced below) which is not marked in accordance with the above reference.  
ANNUAL REPORT #2  
N00014-93-0080  
TITLE: A STUDY OF SOLID  
PROPELLANTS USING A MICROBE MASS  
SPECTROMETER SYSTEM
  3. We request the appropriate distribution statement be assigned and the report returned to DTIC within 5 working days.
  4. Approved distribution statements are listed on the reverse of this letter. If you have any questions regarding these statements, call DTIC's Cataloging Branch, (703) 274-6837.

FOR THE ADMINISTRATOR:

1 Encl

GOPALAKRISHNAN NAIR  
Chief, Cataloging Branch

DISTRIBUTION STATEMENT A:

APPROVED FOR PUBLIC RELEASE: DISTRIBUTION IS UNLIMITED

DISTRIBUTION STATEMENT B:

DISTRIBUTION AUTHORIZED TO U.S. GOVERNMENT AGENCIES ONLY;  
(Indicate Reason and Date Below). OTHER REQUESTS FOR THIS DOCUMENT SHALL BE REFERRED  
TO (Indicate Controlling DoD Office Below).

DISTRIBUTION STATEMENT C:

DISTRIBUTION AUTHORIZED TO U.S. GOVERNMENT AGENCIES AND THEIR CONTRACTORS;  
(Indicate Reason and Date Below). OTHER REQUESTS FOR THIS DOCUMENT SHALL BE REFERRED  
TO (Indicate Controlling DoD Office Below).

DISTRIBUTION STATEMENT D:

DISTRIBUTION AUTHORIZED TO DOD AND U.S. DOD CONTRACTORS ONLY; (Indicate Reason  
and Date Below). OTHER REQUESTS SHALL BE REFERRED TO (Indicate Controlling DoD Office Below).

DISTRIBUTION STATEMENT E:

DISTRIBUTION AUTHORIZED TO DOD COMPONENTS ONLY; (Indicate Reason and Date Below).  
OTHER REQUESTS SHALL BE REFERRED TO (Indicate Controlling DoD Office Below).


DISTRIBUTION STATEMENT F:

FURTHER DISSEMINATION ONLY AS DIRECTED BY (Indicate Controlling DoD Office and Date  
Below) or HIGHER DOD AUTHORITY.

DISTRIBUTION STATEMENT X:

DISTRIBUTION AUTHORIZED TO U.S. GOVERNMENT AGENCIES AND PRIVATE INDIVIDUALS  
OR ENTERPRISES ELIGIBLE TO OBTAIN EXPORT-CONTROLLED TECHNICAL DATA IN ACCORDANCE  
WITH DOD DIRECTIVE 5230.25, WITHHOLDING OF UNCLASSIFIED TECHNICAL DATA FROM PUBLIC  
DISCLOSURE, 6 Nov 1984 (Indicate date of determination). CONTROLLING DOD OFFICE IS (Indicate  
Controlling DoD Office).

The cited documents has been reviewed by competent authority and the following distribution statement is  
hereby authorized.

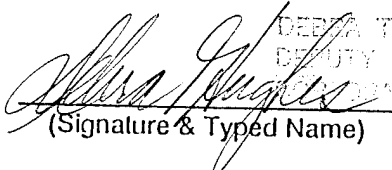
  
(Statement)

OFFICE OF NAVAL RESEARCH  
CORPORATE PROGRAMS DIVISION  
ONE  
300 J. EDGAR HOOVER STREET  
ARLINGTON, VA 22204-4360

\_\_\_\_\_  
(Controlling DoD Office Name)

\_\_\_\_\_  
(Reason)

\_\_\_\_\_  
(Controlling DoD Office Address,  
City, State, Zip)

  
(Signature & Typed Name)

DEBRA T. HUGHES  
DEPUTY DIRECTOR  
CORPORATE PROGRAMS OFFICE

\_\_\_\_\_  
(Assigning Office)

TP 1005  
\_\_\_\_\_  
(Date Statement Assigned)

## Summary

The objective of this work is to determine the chemical mechanisms of solid propellant ignition and deflagration with an emphasis on the decomposition of individual propellant ingredients and on the gas phase reactions of the products of decomposition. A quadrupole mass spectrometer system using quartz microprobes measures species profiles above the surface of the sample during CO<sub>2</sub> laser induced pyrolysis or during laser assisted deflagration of the sample. In addition microthermocouples are used to measure the surface temperature and gas phase temperatures during testing. To complement the experimental studies, chemical kinetic models produced by other researchers are used to model some of the data obtained.

During FY 94, after significant effort to construct the triple quadrupole mass spectrometer (TQMS) and optimize its operational parameters for separation of species at mass 28 (CO, N<sub>2</sub> and C<sub>2</sub>H<sub>4</sub>) and mass 44 (CO<sub>2</sub>, N<sub>2</sub>O and CH<sub>3</sub>CHO) using laboratory standards, it was successfully applied in RDX tests at different pressures and heat fluxes. Using the full capability of the TQMS, two separate tests to quantify the parent and daughter species allow complete determination of the major species in RDX laser assisted deflagration. In addition to the RDX studies, preliminary studies of oxetane polymers were also performed.

The first task for RDX was to determine the relative contributions of species at mass 28 and 44. Mass 28 was found to consist only of N<sub>2</sub> and CO, with no C<sub>2</sub>H<sub>4</sub> present. Throughout the gas-phase, N<sub>2</sub> was generally slightly larger than CO. Mass 44 was exclusively composed of N<sub>2</sub>O and CO<sub>2</sub>. N<sub>2</sub>O constituted all of mass 44 at the surface, but decreased gradually to zero at the end of reaction zones. The opposite was true for CO<sub>2</sub>. Some unknown species above mass 40 were found, and they were identified as HNCO, NH<sub>2</sub>CHO and HONO at mass 43, 45 and 47, respectively. Their signal intensities were not negligible near the surface, especially that of HNCO.

The RDX results at high heat flux and atmospheric pressure show NO and NO<sub>2</sub> profiles that are in good agreement with the recent measurements of Parr and Hanson-Parr obtained by absorption. However, the TQMS data still show a substantial amount of formaldehyde, based upon the 29 amu peak, while Parr and Hanson-Parr detected none in their study. Therefore, additional RDX studies were performed to determine whether other species were contributing to 29 amu. These studies showed that near the surface another species was contributing to the signal at 29 amu. Further tests to determine the exact structure of the unknown peak at mass 29 will be a priority in the near term.

The effects of heat flux and pressure were also studied for RDX laser-assisted combustion. By increasing heat flux and decreasing pressure, reaction zones were stretched out, but the major reaction pathways of decomposition were found to be unaffected. The primary flame zone was marked by the disappearance of mass 29 and NO<sub>2</sub>, and the production of NO, CO, CO<sub>2</sub> and H<sub>2</sub>O. In the secondary flame zone, HCN, NO and to a lesser extent N<sub>2</sub>O were consumed, and CO<sub>2</sub>, N<sub>2</sub>, CO, H<sub>2</sub>O and H<sub>2</sub> were produced. No evidence of a near surface reaction zone, postulated by Russian researchers, was found very near the surface and preceeding the primary flame zone even at the low pressure and high heat flux condition.

In addition to the RDX tests, experiments were performed to study the parent ions produced by oxetane polymers, BAMO and NMMO. These results show more than fourteen major species over a rather narrow molecular weights from 15 to 45. The presence of so many species at close molecular weights presents a substantial challenge to the TQMS. As a result significant effort will be required to determine the structure of these species using the full capabilities of the TQMS.

<input checked="checked" type="checkbox"/>	
<input type="checkbox"/>	
<input type="checkbox"/>	
per attach	
Distribution/	
Availability Codes	
Dist	Avail and/or Special
A-1	

## **Objective**

The objective of this effort is to determine the chemical mechanisms of solid propellant ignition and deflagration with an emphasis on the decomposition of individual propellant ingredients and on the gas phase reactions of the products of decomposition. The information gained will be coupled into existing modeling efforts supported by ONR. In this program both solid oxidizers and energetic binders will be studied. A quadrupole mass spectrometer system using quartz microprobes is used to measure species profiles above the surface of the sample during CO<sub>2</sub> laser induced pyrolysis or during laser assisted deflagration of the sample. Gas phase temperature profiles are measured with micro-thermocouples no larger than 50 micron.

During the past year a related objective of the program was to bring the (MPMS) system with the triple quadrupole mass spectrometer (TQMS) to a fully operational state. The TQMS can detect and quantify species with similar molecular weights but different compositions, and identify the structure of unknown species. This objective was achieved early in FY 94.

## **Approach**

A schematic diagram of the experimental setup is given in Fig. 1. The energy source of ignition was a high-power CO<sub>2</sub> laser with a maximum continuous wave power of 700W. The laser beam passed through a mask and an expanding lens before entering the test chamber through a KCl window. The size of beam was selected to be about twice that of the sample so that a nearly uniform beam profile could be applied to the surface. The RDX samples were 0.64 cm diameter pellets pressed from RDX powder.

The propellant samples were glued to a small block angled at 45° to the incident laser beam so that the sampling microprobe approached the sample perpendicular to the center of the sample surface. During a test, the sample was pushed toward the sampling probe by a linear positioner to obtain species profiles. A high-quality plexi-glass window was installed on one side of the chamber for video photography of the flame and the RDX pellet. The video was acquired using a CCD video camera with a micro lens; after each test it was used to identify the sampling height, i.e., the distance between the RDX surface and the sampling probe tip. Typically, a magnification of 30 to 40 times was used which produced a spatial resolution of about 20mm for the videos.

The analysis of gaseous species was performed using the microprobe/mass-spectrometer (MPMS) system. The species were sampled by quartz microprobe with an orifice diameter of 20 to 30mm which produced spatial resolution of 100 to 150 mm. The sample gases were drawn through the probe and into the mass spectrometer by a set of turbomolecular pumps

and vacuum pumps and ionized at the ionizer in MS. In early experiments to determine the decomposition species a single quadrupole mass spectrometer was used. In later tests for species profiles the mass spectrometer unit was upgraded to a triple quadrupole mass-spectrometer (TQMS) from Extrel. The TQMS was required for these tests to overcome difficulties in differentiating species with same mass using the single quadrupole mass spectrometer. Differentiating multiple species with the same mass is very difficult with a single quadrupole and requires multiple runs at different ionization energies or the application of a matrix approach to obtaining quantitative data. Using the so-called "daughters" mode of operation of the TQMS, it was possible to identify and differentiate  $N_2$ , CO,  $C_2H_4$  at 28-amu, NO,  $CH_2O$  at 30-amu, and  $N_2O$ ,  $CO_2$  at 44-amu as well as possible species at 29-amu.

In the daughter mode of operation, the mass of interest, often referred to as the "parent", is selected in the first quadrupole. The parent ions then enter the second quadrupole (Q2) and are fragmented into smaller species, the "daughters", by the process of collision-induced dissociation (CID) with an inert gas separately supplied into Q2. Argon was used as the collision gas in this study to minimize its contribution to fragmented masses. The daughters, at masses less than their parent, are detected in the third quadrupole. For complex parent ions, some of the daughters might overlap if the parents contain common structures. In the present study, however, at least one unique daughter could be acquired for each parent.

Several methods of calibration were used to obtain the sensitivity coefficients (intensity/concentration) of each species. Most stable species were calibrated directly with the gas mixtures of known concentration. To calibrate water, water vapor was acquired from liquid water which was vaporized by the  $CO_2$  laser. Paraformaldehyde and trioxane, polymeric forms of  $CH_2O$ , were used for its calibration. They were also vaporized with the  $CO_2$  laser to obtain gas-phase formaldehyde. Typically the sensitivity factors were repeatable within 10%. The calibration of species for which standards were not readily available, e.g. HCN, were estimated by correlating the signal intensity to that of calibrated species with a similar appearance potential through the ratio of their cross-sections.<sup>1</sup>

For all of the calibrations and in the actual tests, an ionization energy of 22 eV was used to minimize fragmentation of molecules and to get acceptable intensities. However, this setting was still high compared to the ionization energies of 9 -15 eV for most organic compounds, thus some fragments were formed and contributed to the signals at masses other than the parent mass. In such instances, these signals were subtracted from the mass signal of interest.

In reducing the experimental data the measured concentrations were totaled and each concentration was divided by the total to get the mole fractions of the sampled gases. This method of calculating normalized mole fractions eliminates the effect of sample temperature

on the observed signal intensities since the temperature dependence cancels out. This calculation method also cancels out the effect on signal intensity of probe orifice blockage during a test. The measured mole fractions were then used to perform element balances through the reaction zones as a check on the quality of the data.

### **Summary of Results**

This section of the report will provide more details on the three major areas of study for FY 94. They are studies to determine the contributions of various species at 28 and 44 amu as well as 29 amu, experiments to determine the effects of heat flux and pressure on RDX gas-phase structure, and preliminary studies of the oxetane polymer, BAMO/NMMO.

### **RDX Experimental Studies**

#### **Species at 28 and 44 amu**

In RDX combustion, possible sources of mass 28 are  $N_2$ , CO and  $C_2H_4$ . Using the TQMS, these three species could be differentiated and identified in the daughter mode. Q1 was fixed at mass 28 and Q3 was scanned over possible masses of daughters in each species. By this method,  $N_2$  was identified by mass 14 (N), CO was by 12 (C), and  $C_2H_4$  by 15 ( $CH_3$ ). For  $C_2H_4$ , the signal intensities of mass 27 ( $C_2H_3$ ), 26 ( $C_2H_2$ ), 25 ( $C_2H$ ) and 14 ( $CH_2$ ) should be higher than that of mass 15 ( $CH_3$ ) because they are easier to create by fragmentation than mass 15. However, mass 25 to 27 were too near to the parent mass 28 to identify because of the high signal level from the parent, and mass 14 overlapped with the daughter mass from  $N_2$ . In the actual experiment, the signal of mass 15 was just above the noise range, thus  $C_2H_4$  appears not to be a major product of RDX. Without  $C_2H_4$  present,  $N_2$ , CO were easily distinguished in the daughter mode.

Three possible species could exist at mass 44:  $N_2O$ ,  $CO_2$  and  $CH_3CHO$ . As in the case of mass 28, key daughters were identified during calibration for each of these species: mass 28 ( $N_2$ ) and 30 (NO) for  $N_2O$ , mass 28 (CO) for  $CO_2$ , and primarily mass 15 ( $CH_3$ ) and 29 (CHO) for  $CH_3CHO$ . In the actual experiments, no daughter signals were found except mass 28 and 30 by screening from mass 10 to 40 in the daughter mode, thus  $CH_3CHO$  was eliminated as a possible product. Actually this result was expected because formation of  $CH_3CHO$  in RDX combustion requires complex interactions. It is interesting to note that  $CH_3CHO$  is found, however, in RDX-based composite propellants<sup>2</sup>. The daughter signal at mass 28 can come from  $N_2O$  and  $CO_2$ , simultaneously. Therefore, mass 30 was selected exclusively to identify  $N_2O$ , and  $CO_2$  could be easily identified by subtracting the intensity of  $N_2O$  from the total intensity of mass 44 signal in the parent mode.

The trends of N<sub>2</sub>O and CO<sub>2</sub> versus height from the surface are shown in Figure 2 at three test conditions. N<sub>2</sub>O constitutes all of mass 44 at the surface without the existence of CO<sub>2</sub>, but N<sub>2</sub>O decreases exponentially as the height increased. At the end of reaction zones, all of mass 44 was composed of CO<sub>2</sub>, one of the final products of combustion. From the profiles of the N<sub>2</sub>O species, the expansion of reaction zones as heat flux increased and pressure decreased is clearly visible.

#### Species at high masses 43, 45 and 47

Species at masses 43, 45 and 47 were identified in several previous studies and were recognized to have important roles in the gas-phase chemistry of RDX.<sup>3,4,5,6,7</sup> Mass 43 was identified as HNCO, mass 45 as NH<sub>2</sub>CHO and mass 47 as HONO. In the present study, the intensities of these species became larger as pressure decreased and heat flux increased, i.e. as the reaction zones expanded. The mole fractions of HNCO at the surface, however, were almost constant in the range of 3.5 % - 4.5 % for all experimental conditions. The sensitivity of HNCO here was estimated by the theory of ionization cross section<sup>1</sup> referred in the experimental section.

#### Species at 29 amu

Some questions have been raised regarding the mole fraction of CH<sub>2</sub>O near the surface of deflagrating RDX obtained from mass 29. The mole fraction of CH<sub>2</sub>O has been reported to be almost zero near the surface in other studies.<sup>8,9</sup> In these studies, the ranges of experimental conditions were not too different from those of the present study and therefore experimental conditions cannot explain the differences. Based upon the signal at mass 29 in previous work with the MPMS<sup>10,11</sup>, the mole fraction was measured to be about 7 % in 1 atm and 100 W/cm<sup>2</sup>, and about 18 % in 0.5 atm and 400 W/cm<sup>2</sup> at the surface. The discrepancy between these results and those of other researchers required careful consideration of possible causes.

Several possible reasons difference related to the probe sampling method were originally considered as possible causes. One of possible reasons was the condensation of some CH<sub>2</sub>O in the microprobe or vacuum chamber with subsequent evaporation. Another possible one was that there were other species at mass 29 besides CHO. The second possibility was more reasonable because the microprobe sampling method had problems only in detecting CH<sub>2</sub>O/CHO, not any other major product. This possibility supplied the motivation to perform experiments in the daughter mode for the parent at mass 29 and 30.

The results of calibration in daughter mode for NO, CHO and CH<sub>2</sub>O at 1 atmosphere are shown in Figure 3. Mass 14 (N) and 16 (O) were detected with the ratio of ~1.65 to 1 for



NO. For CHO, mass 13 (CH) and 12 (C) were identified with the ratio of  $\sim 2.4$  to 1, and for CH<sub>2</sub>O mass 14 (CH<sub>2</sub>), 13 (CH) and 12 (C) with the ratio of  $\sim 20 : 2.5 : 1$ . In experiments with RDX at 1 atm and 100 W/cm<sup>2</sup>, several interesting results were acquired in terms of mass 29 and 30. In Figure 4-(a), daughter masses 14 and 16 were measured for the parent mass 30, and the ratio of mass 14 and 16 was calculated. In the region where the mass 30 is large, the ratio was within the bounds of 1.6 and 1.73. Comparing this ratio to the calibration of Figure 3 suggests that the amount of CH<sub>2</sub>O is small or the ratio would deviate from the NO calibration data due to the presence of a strong 14 signal from CH<sub>2</sub>O. Based upon these results, the maximum possible mole fraction of CH<sub>2</sub>O near the surface was about 3 %. Considering the inevitable fluctuation of signals in calibration and actual experiments in daughter mode of TQMS, it is possible that CH<sub>2</sub>O does not exist near the surface at this test condition. More experiments will be performed at other conditions to ascertain whether CH<sub>2</sub>O is present.

Results from actual experiments at mass 29 and 30 are also given in Figure 4. From the calibration of CHO, mass 13 and 12 were identified as the only possible daughters if only CHO existed at mass 29. In the real test at 1 atm and 100 W/cm<sup>2</sup>, however, a large signal at mass 14 was detected near the surface. Possible chemical species should be just CH<sub>2</sub> or N for mass 14, which could come from other parent masses such as H<sub>2</sub>CNH or C<sub>2</sub>H<sub>5</sub>, a radical which would have to come from fragmentation of a larger species in the ionizer. C<sub>2</sub>H<sub>5</sub> was eliminated as a possible species because mass 15 (CH<sub>3</sub>) is formed in its fragmentation, and mass 15 was not detected in daughter mode. Therefore, the most likely species appears to be something containing N, such as H<sub>2</sub>CNH. The fragment of mass 14 is highly possible from H<sub>2</sub>CNH, because CID is strong enough to break multiple bonds and thus no preference was identified in the fragmentation of parent ions<sup>1</sup>. However, while the radical H<sub>2</sub>CN has already been suggested as an important intermediate species to form HCN<sup>3</sup>, H<sub>2</sub>CNH has never been reported in other experiments. Thus any firm conclusion about mass 29 must be delayed until more decisive evidence can be found for the existence of H<sub>2</sub>CNH.

#### Effects of Heat Flux and Pressure on RDX Gas-phase Structure

Measurements of major species at the condition of 1 atm and 100 W/cm<sup>2</sup> are shown in Figure 5. Several experiments were actually conducted at this condition to increase the resolution of sampling. Increasing resolution was achieved by changing the starting height of sampling probe, because the quartz microprobes were found not to withstand more than 400 msec outside flame zones without melting. Figure 6 is a combination of two results with different starting heights; the results were cross-checked with other results at same condition to validate measured mole fractions.

Decomposition chemistry in the gas-phase starts by the disappearance of mass of 29 and  $\text{NO}_2$  in the primary flame zone very near the surface. Primary products of this consumption were  $\text{H}_2\text{O}$ ,  $\text{NO}$ ,  $\text{CO}$  and  $\text{CO}_2$ .  $\text{H}_2$  was relatively inert in this zone. The existence of  $\text{N}_2$  from the surface should not be overlooked. Its production was almost unaffected by the change of pressure and heat flux.

The secondary flame zone has been characterized by the consumption of  $\text{NO}$  and  $\text{HCN}$ , and by the production of  $\text{CO}_2$ ,  $\text{N}_2$ ,  $\text{CO}$ ,  $\text{H}_2\text{O}$  and  $\text{H}_2$ . The consumption of  $\text{N}_2\text{O}$  produces  $\text{N}_2$  in this zone. At approximately 3mm from the surface, the reaction zone came to the post-flame region at this condition. In the region, major products were identified as  $\text{CO}_2$ ,  $\text{N}_2$ ,  $\text{CO}$ ,  $\text{H}_2\text{O}$ ,  $\text{H}_2$  and small amount of  $\text{NO}$  ( $\sim 2\%$ ). Small signal intensities of  $\text{N}_2\text{O}$ ,  $\text{NO}_2$ ,  $\text{HCN}$  were noticed in this region, but they are in the range of noise fluctuation.

In Figure 6, the species profiles are shown for a heat flux of  $400 \text{ W/cm}^2$  at 1atm. Chemical structures of flame were similar to those at  $100 \text{ W/cm}^2$ . However, the end of the secondary flame zone expanded to more than 5mm from the surface based upon the profile of  $\text{NO}$ . At the surface, mole fractions of  $\text{NO}_2$  and  $\text{HCN}$  increased and that of  $\text{N}_2\text{O}$  decreased relative to the lower heat flux case, because the N-N bond scission was preferred at the high heat flux condition. The thickness of primary reaction zone, indicated by the  $\text{NO}_2$  profile, was not changed as heat flux increases. This trend was also observed for other species in Figure 6 and shows that the change of heat flux does not have much effect on the chemical mechanisms near the surface. From the profiles of major species, especially  $\text{NO}$ ,  $\text{N}_2\text{O}$  and  $\text{HCN}$ , the secondary flame zone was also stretched substantially compared with that at  $100 \text{ W/cm}^2$ . Even at 5mm from the surface,  $\text{NO}$  and  $\text{HCN}$  were still being consumed.

The species profiles in the gas-phase at the condition of 0.5atm and  $400 \text{ W/cm}^2$  are presented in Figure 7. Because effects of lower pressure and higher heat flux were added in the experiment, the reaction zone near the surface was highly stretched. Therefore, the secondary flame zone did not begin until about at 4.5 mm from the surface, as indicated by the consumption of  $\text{NO}$  and  $\text{HCN}$ . The existence of another reaction zone very near the surface, postulated by Korobeinichev et al.<sup>8</sup> is not evident in the species profiles of products  $\text{NO}_2$ ,  $\text{HCN}$  and  $\text{CH}_2\text{O}$ . Mole fractions of these species showed practically no change near the surface, suggesting that the additional effect of lowering pressure from 1 to 0.5 atm was only stretching the reaction zone near the surface. The mole fraction of mass 29 and  $\text{NO}_2$  increased and  $\text{HCN}$  decreased with little change in  $\text{N}_2\text{O}$  at the surface in the comparison to results of 1 and 0.5 atm.

The primary flame zone was stretched up to 3 - 3.5 mm and secondary flame zone reactions started at 4 - 4.5 mm.  $\text{HCN}$  and  $\text{NO}$  were identified to be the only species produced in the primary flame zone again. At this condition, the primary reaction thickness increased

to ~4 mm from ~0.5 mm of previous two conditions. This result shows that pressure is the primary means to expand reaction zones near the surface. Reaction mechanisms appear to be quite the same as that of previous two conditions, thus stretching the reaction zones by increasing heat flux and decreasing pressure appear to be a valid means to study the gas-phase.

Modeling of the high heat flux results is underway and the results are targeted for a refereed journal publication.

### **Oxetane Polymer Studies**

In addition to the RDX tests, experiments were performed to study the parent ions produced by oxetane polymers, BAMO and NMMO. These results show more than fourteen major species over a rather narrow molecular weights from 15 to 45. The presence of so many species at close molecular weights presents a substantial challenge to the TQMS. As a result significant effort will be required to determine the structure of these species using the daughters mode. Once these species have been identified, the polymer will be used in sandwich studies.

### **Future Work**

#### **MPMS studies**

During the next fiscal year efforts will concentrate on the identification of the unknown species at 29 amu in RDX and the work on RDX will be prepared for submission to a refereed journal. Following the completion of the RDX studies, experiments to identify the species produced by the oxetane polymers will be carried out. Also preliminary "sandwich" studies will be performed.

#### **Microthermocouples**

Recently Professor Zenin of Russian Institute of Chemical Physics visited Penn State and presented a series of seminars on his thermocouple methods. These methods will be adapted to be used in the MPMS facility so that temperature profiles can be obtained for in the condensed and gas-phases of RDX.

#### **RDX Modeling Studies**

In the very near future the RDX results at 400 W/cm<sup>2</sup> will be combined with the temperature profile of Parr and Hanson-Parr and used to validate the kinetics model of Yetter and Dryer with the CHEMKIN code.

## References

1. Bobeldijk, M., Van der Zande, W. J., and Kistemaker, P. G., "Simple models for the calculation of photoionization and electron impact ionization cross sections of polyatomic molecules", *Chemical Physics*, 1994, 179, pp. 125-130; Margreiter, D., Deutsch, H., Schmidt, M., and Märk, T. D., "Electron Impact Ionization Cross Sections of Molecules", *International Journal of Mass Spectrometry and Ion Processes*, 1990, 100, pp. 157-176.
2. Tang, Ching-Jen, Lee, YoungJoo, and Litzinger, Thomas A., "A Study of Gas-phase Processes during the Deflagration of RDX Composite Propellants using a Triple Quadrupole Mass-spectrometer", 31th JANNAF Combustion Meeting, 1994
3. Behrens, R. Jr, and Bulusu, S., "Thermal Decomposition of Energetic Materials 3. Temporal Behavior of the Rates of Formation of the Gaseous Pyrolysis Products from Condensed-Phase Decomposition of 1,3,5-Trinitrohexahydro-s-triazine", *J. Phys. Chem.*, 1992, 96, pp. 8877-8891.
4. Melius, C. F., "The Gas Phase Flame Chemistry of Nitramine Combustion", 25th JANNAF Combustion Meeting, 1988, pp. 155-162.
5. Oyumi Y., and Brill, T. B., "Thermal Decomposition of Energetic Materials 3. A High-Rate, In Situ, FTIR Study of the Thermolysis of RDX and HMX with Pressure and Heating Rate as Variables", *Combustion and Flame*, 1985, 62, pp. 213-224.
6. Brill, T., "Surface Chemistry of Energetic Materials at High Temperature", *Mat. Res. Soc. Symp Proc.*, Vol. 296, 1993, pp. 269-280.
7. Melius, C. F., "Thermochemical Modeling: I. Application to Decomposition of Energetic Materials", *Chemistry and Physics of Energetic Materials*, Bulusu, S. N. Eds., 1990, pp. 21-49.
8. Korobeinichev, O. P., Kuibida, L. V., Orlov, V. N., Tereshchenko, A. G., Kutsenogii, K. P., Mavliev, R. V., Ermolin, N. E., Fomin V. M., and Emel'yanov I. D., "Mass Spectrometric Probe Study of the Flame Structure and Kinetics of Chemical Reactions in Flames", *Mass-Spektrom. Khim. Kinet.*, 1985, pp. 73-93.
9. Hanson-Parr D., and Parr, T., "RDX Flame Structure", The proceedings of the 25th International Symposium of Combustion (the Combustion Institute), 1994.
10. Fetherolf, B. L., and Litzinger, T. A., "Chemical Structure of the Gas phase Above Deflagrating RDX: Comparison of Experimental Measurements and Model Predictions", 30th JANNAF Combustion Meeting, November 1993.
11. Fetherolf, B. L., Liiva, P. M., Litzinger, T. A., and Kuo, K. K., "Thermal and Chemical Structure of the Preparation and Reaction Zones for RDX and RDX composite Propellants", 28th JANNAF Combustion Meeting, CPIA Publ. 573, Vol. II, October 1991, pp. 379-386.

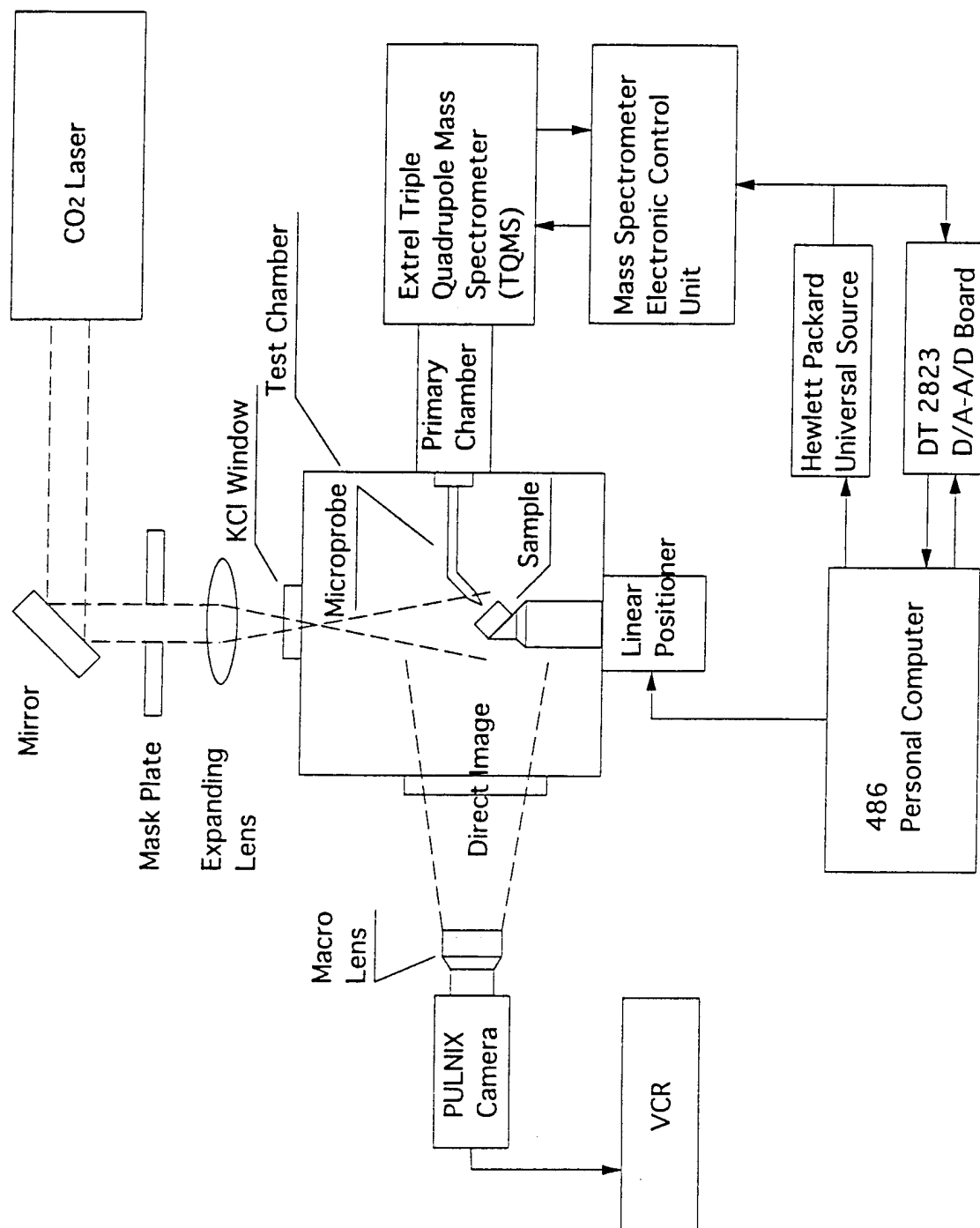


Figure 1. Overall Experimental Setup for the studies of RDX propellants in the gas phase reactions using microprobe/triple quadrupole mass spectrometer(TQMS)

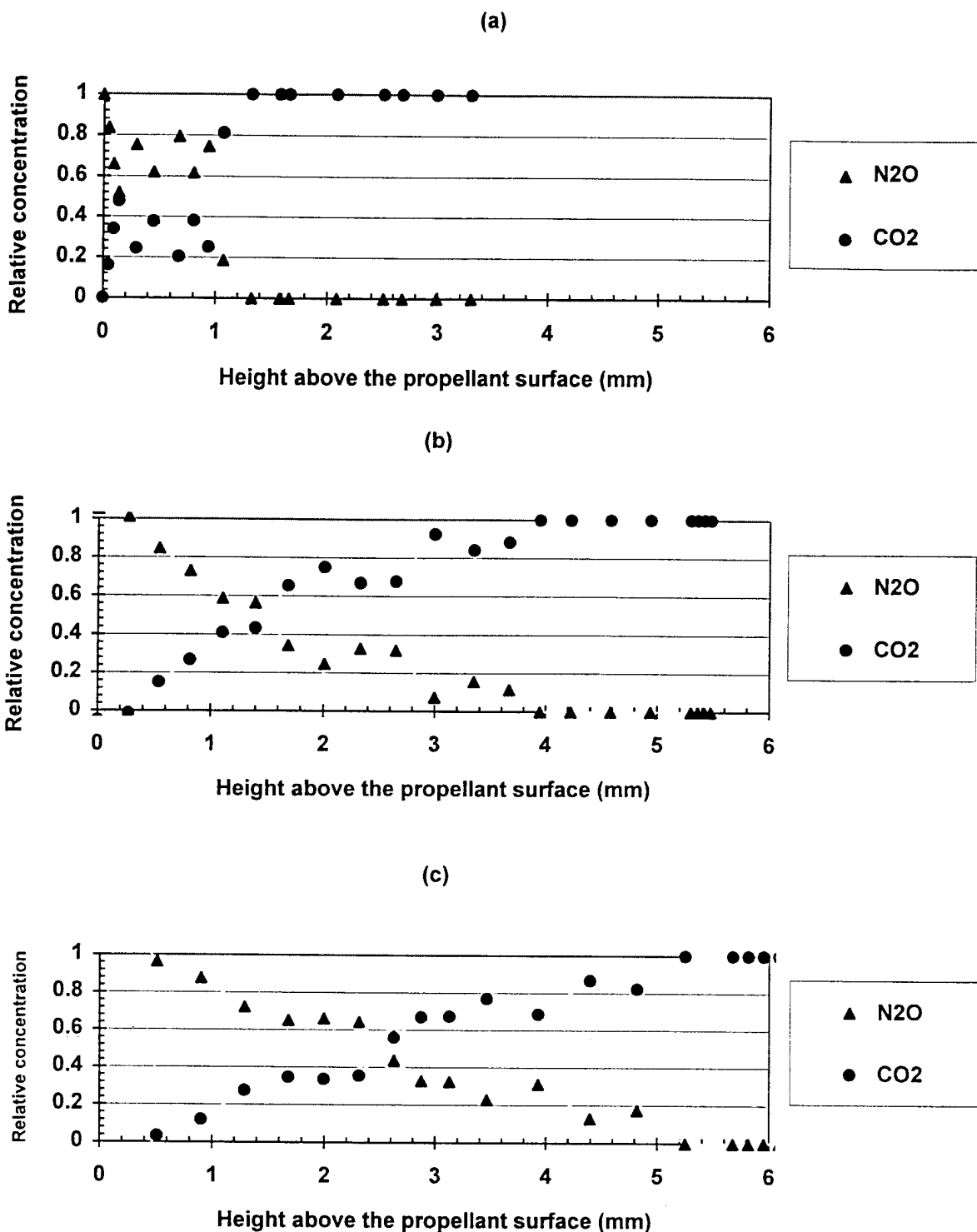


Figure 2. 44 amu split between CO<sub>2</sub> and N<sub>2</sub>O for (a) 1 atm and 100 Wcm<sup>2</sup>, (b) 1 atm and 400 Wcm<sup>2</sup> and (c) 0.5 atm and 400 Wcm<sup>2</sup>.

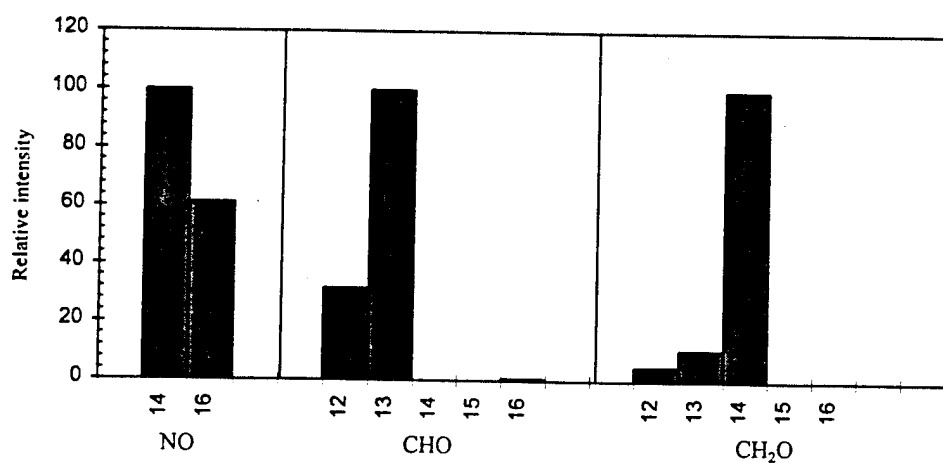


Figure 3 Intensities of daughter ion signals for the calibration of parent NO, CHO, and CH<sub>2</sub>O. All tests were performed at 1atm and in N<sub>2</sub> environment.

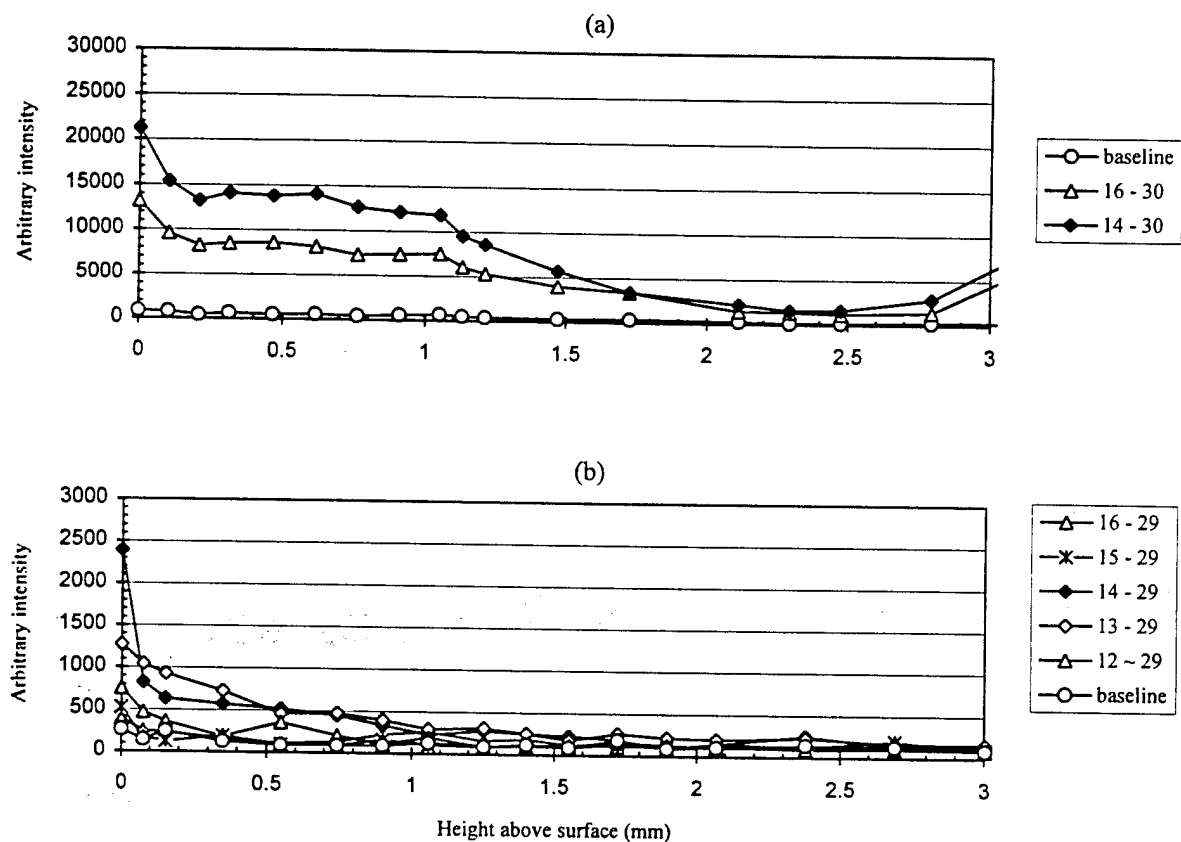


Figure 4 Intensities of daughter ion signals in the conditions of 1atm and 100 W/cm<sup>2</sup> for (a) mass 30 and (b) mass 29.

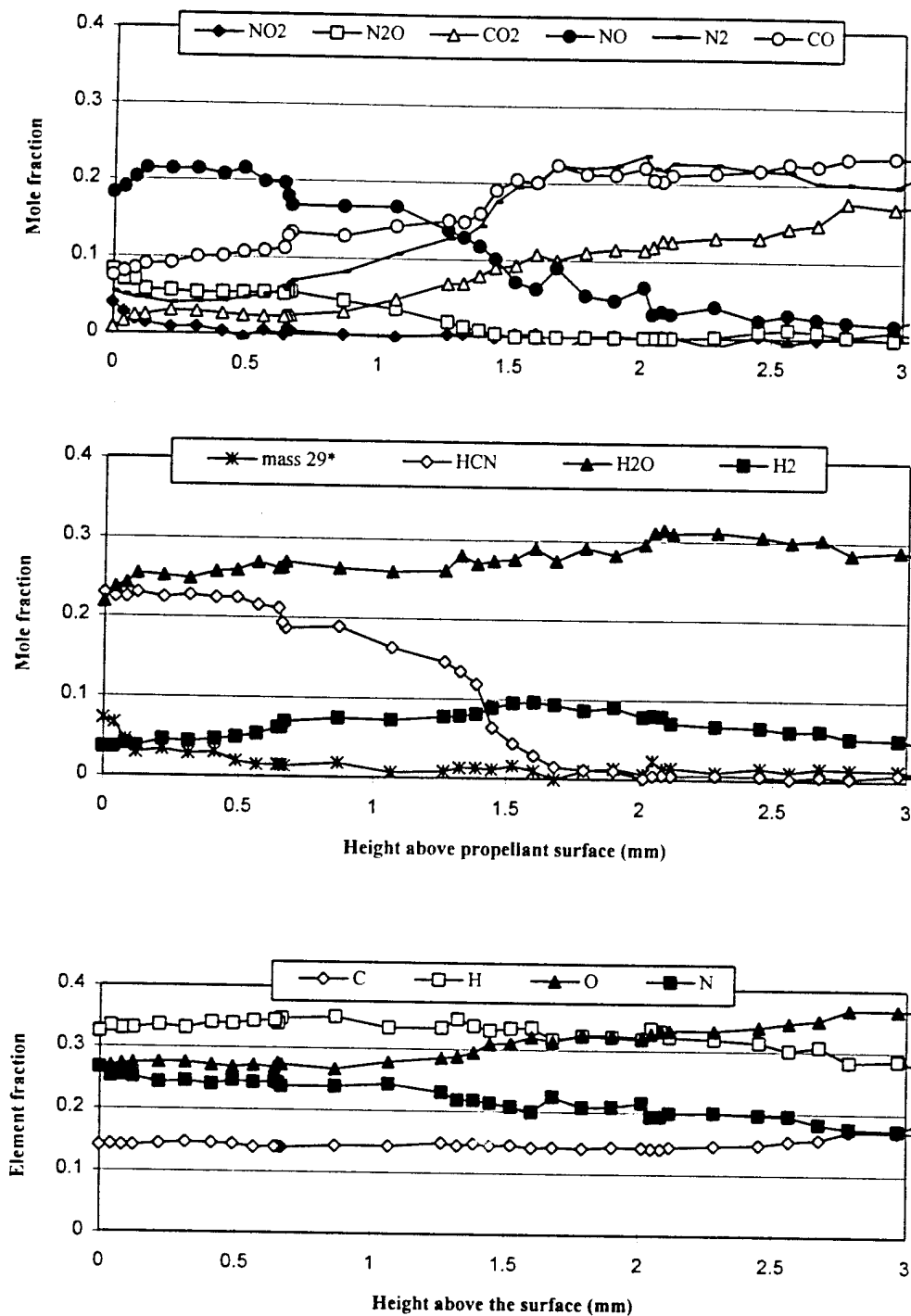


Figure 5. Species profiles and element fractions for RDX at 1 atm and 100 Wcm<sup>2</sup>. (\*here 29 amu was reduced using the calibration factor for H<sub>2</sub>CO)



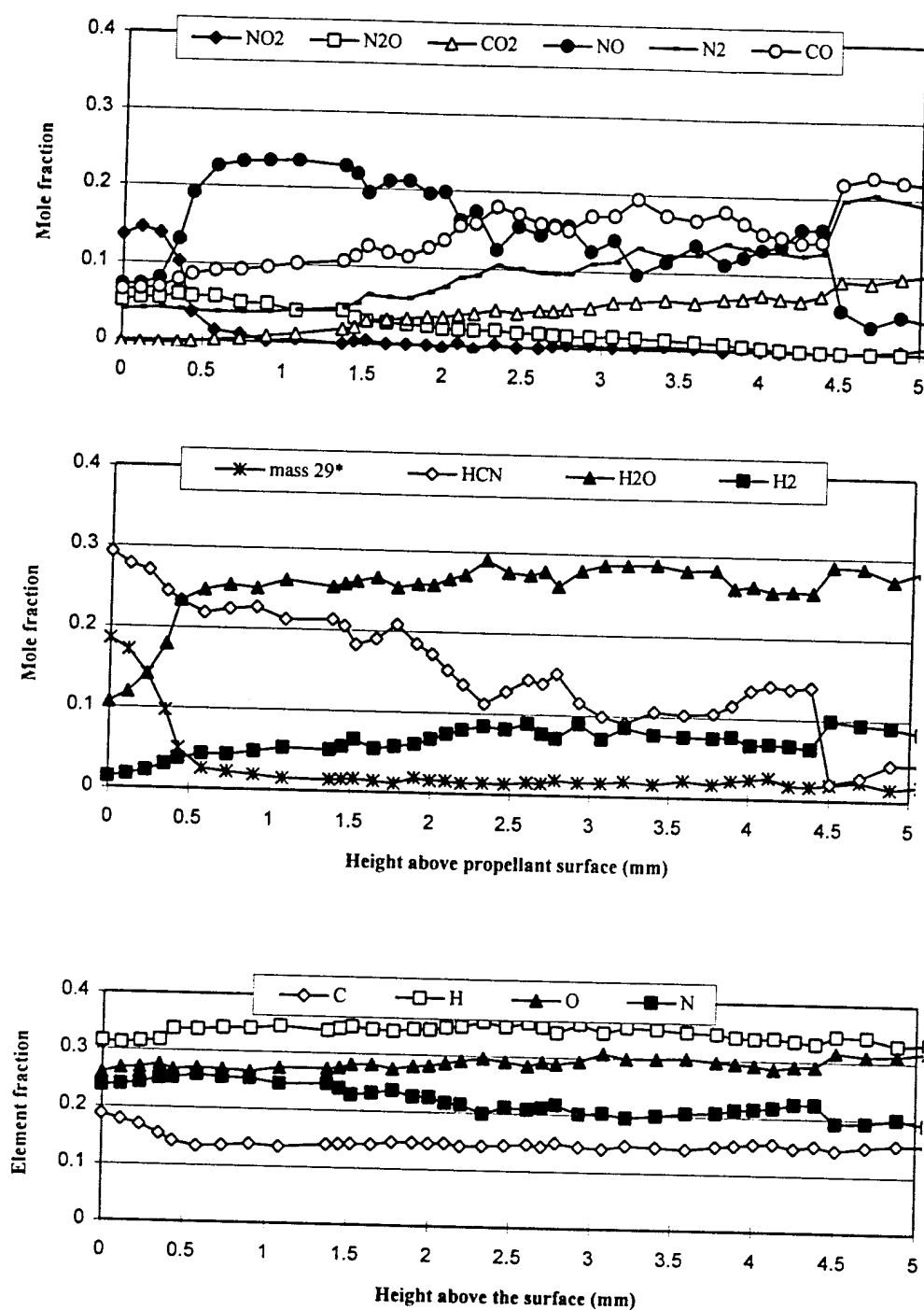


Figure 6. Species profiles and element fractions for RDX at 1 atm and 400 W/cm<sup>2</sup>. (\*here 29 amu was reduced using the calibration factor for H<sub>2</sub>CO)

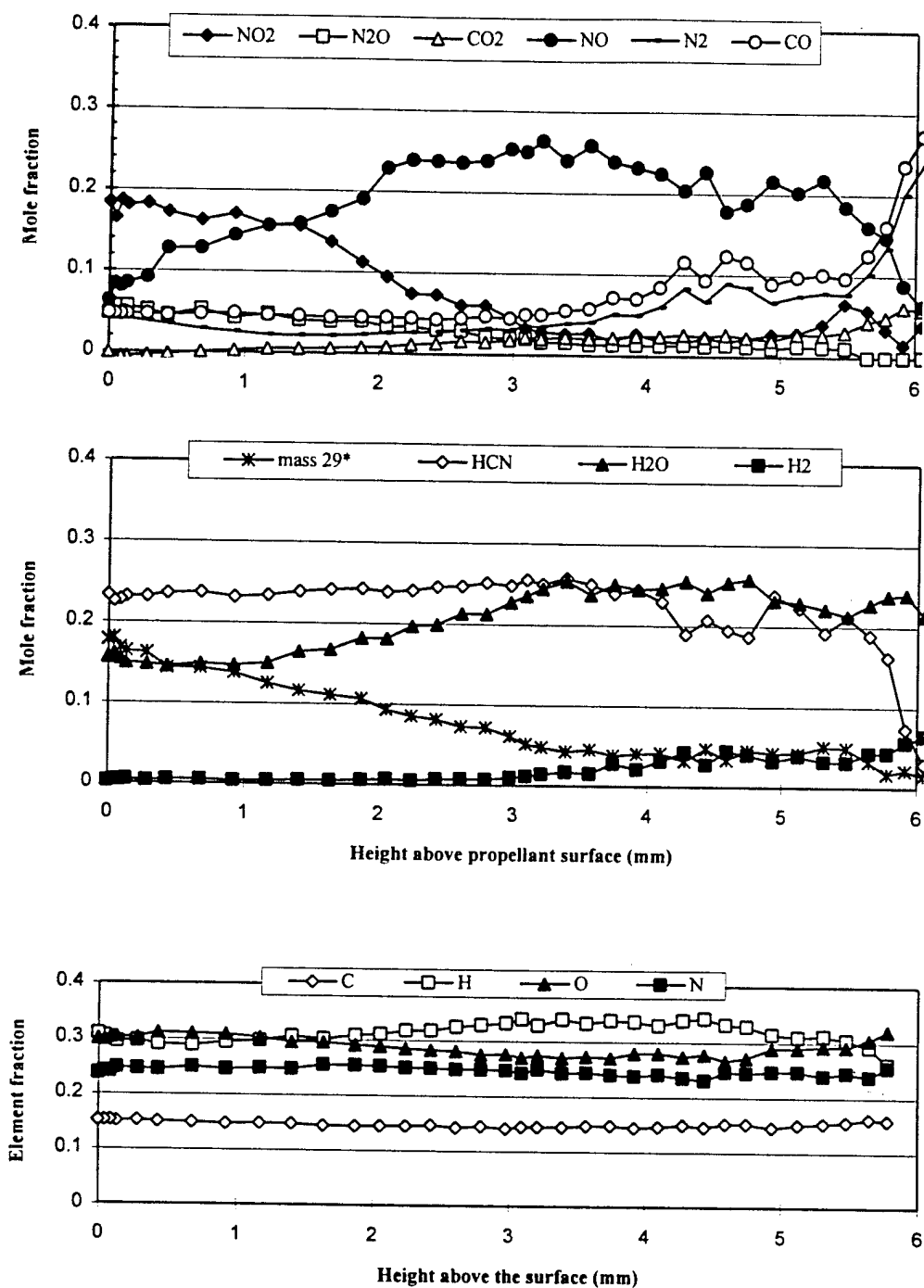


Figure 7. Species profiles and element fractions for RDX at 0.5 atm and 400 W/cm<sup>2</sup>. (\*here 29 amu was reduced using the calibration factor for H<sub>2</sub>CO)